

Nonuniversality in level dynamics

Paweł Kunstman, Karol Życzkowski, and Jakub Zakrzewski

Instytut Fizyki Mariana Smoluchowskiego, Uniwersytet Jagielloński, ulica Reymonta 4, 30-059 Kraków, Poland

(Received 7 October 1996)

Statistical properties of parametric motion in ensembles of Hermitian banded random matrices are studied. We analyze the distribution of level velocities and level curvatures as well as their correlation functions in the crossover regime between three universality classes. It is shown that the statistical properties of level dynamics are in general *nonuniversal* and strongly depend on the way in which the parametric dynamics is introduced. [S1063-651X(97)04803-4]

PACS number(s): 05.45.+b, 95.10.Fh, 47.52.+j

I. INTRODUCTION

A link between random matrix theory (RMT) [1] and the statistical properties of spectra of quantum systems is well established. Depending on the symmetry of a classically chaotic quantum system, its spectral fluctuations are described by the Gaussian orthogonal (GOE), the Gaussian unitary (GUE), or the Gaussian symplectic ensemble (GSE) [2,3].

Quite often the physical systems depend on some external parameter, say, λ ; therefore, it is interesting to study the level dynamics, i.e., the motion of eigenvalues $E_i(\lambda)$ as a function of λ . Among the first parametric properties studied were the investigations of the avoided crossings gaps [4–6], the parametric number variance [7], or the curvature of the levels (i.e., the second derivatives of their energies with respect to the parameter) [8–13]. It has been claimed that the statistical properties of level dynamics are universal for disordered or strongly chaotic systems [8,14] provided the change of λ does not modify global symmetries properties. To reveal the universality one has to both unfold the energy levels [3] and appropriately rescale the parameter λ [8,11,14]. Other statistical measures of parametric dynamics such as the level slope (velocity) distribution (Gaussian shaped for random systems [8,11,14]), the velocity-velocity correlation function [14–17] in the bound spectrum, or parametric conductance fluctuations [18] and fluctuations in the Wigner time delay [19] for scattering systems have also been discussed.

A word of caution is, however, necessary at this point. Even for the nearest-neighbor spacing distribution, widely considered to be universal, exceptions from the RMT prediction may be quite significant for real physical systems [20]. Much more pronounced and common are the deviations from the RMT predictions for the parametric motion of levels. In particular, as shown by Takami and Hasegawa [10], the curvature distribution shows nonuniversal behavior for small curvatures even for the mixing system (a Bunimovich stadium). Similarly, non-Gaussian slope distributions as well as strongly non-Cauchy-like curvature distributions were observed for a magnetized hydrogen atom [11]. The origin of these deviations has been linked to partial wave-function localization on unstable periodic orbits. Thus the nongeneric features of parametric statistics may provide most interesting information about the physics of a given physical system.

Most of these studies considered pure symmetry cases,

i.e., systems pertaining to a given, e.g., GOE universality class. This is often not the case in a realistic situation. In particular, in the presence of the magnetic field or the Aharonov-Bohm flux, the time-reversal invariance (TRI) symmetry becomes broken; such a situation corresponds to a crossover between the GOE and the GUE for a random system. In this context the velocity-velocity correlation function has been studied intensively [21,22,17] as well as the velocity distribution [23] or the curvature distribution [24,25]. The authors considered mostly the situation when the increase of the external parameter λ (e.g., the magnetic field) destroys the time-reversal invariance, although, importantly, it has been noticed [23] that the parametric velocity distribution may strongly depend on the nature of the perturbation. Relatively less frequent were studies of the parametric dynamics in the transition region between completely delocalized and localized spectra (see, however, e.g., the treatment of the velocity distribution for the broken-TRI-symmetry case in [26,27]).

In order to model the spectra of quantum systems in a crossover regime (a weak localization or a partially broken symmetry) one may utilize random matrix ensembles that interpolate between the canonical ensembles. For example, real symmetric band random matrices are capable of modeling the transition between the localized and the delocalized regime. Statistical properties of their eigenvalues and eigenvectors depend on a single scaling parameter $x = b^2/N$ [28], where N denotes the matrix size and b the bandwidth. Allowing the matrices to be Hermitian and changing the relative weight of the imaginary component α , one can model the effect of the time-reversal symmetry breaking and the transition from an orthogonal to a unitary universality class. The corresponding scaling parameter y is proportional to $N\alpha$ [29] for small perturbations. An ensemble of Hermitian band random matrices (HBRMs) can therefore be completely characterized by two scaling parameters (x,y) [30]. The Poissonian, strongly localized spectrum is obtained in the limit $x \ll 1$, while in the opposite delocalized limit $x \gg 1$ the model reduces to the GOE for $y=0$ and the GUE for $y \gg 1$.

This work is intended as a systematic study of the parametric dynamics and the corresponding statistical measures in the transition region and in the localized regime. Our work differs from most of the analyses mentioned above in the way the parametric dependence is introduced. We assume

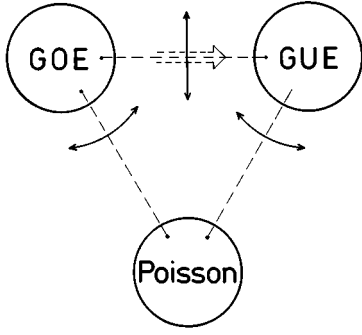


FIG. 1. Scheme of the space of random matrices (and dynamical systems). Three circles represent universality classes (Poissonian, orthogonal, and unitary) and dashed lines represent crossovers between them. Solid arrows stand for perpendicular transitions, analyzed in this paper. A broken arrow exemplifies a parallel transition, not treated here.

that the changes of λ leave the global properties of the system unaffected. In the random matrix approach this is equivalent to the assumption that the statistical properties of the ensemble of matrices do not depend on the value of the parameter λ determining the parametric dynamics. For physical system applications this is equivalent to saying that the symmetry properties of the system considered, in addition to the character of the underlying classical dynamics (say, the fraction of the phase-space volume that is chaotic), are invariant with respect to λ or, from a practical point of view, the the dynamics changes only weakly with λ , in the interval of λ values considered in each case. The level dynamics is, in a sense, ‘‘perpendicular’’ to crossovers between canonical ensembles, as schematically shown in Fig. 1. Such a physical situation may correspond to a variation of the disorder parameter in a mesoscopic system, for which all other parameters are kept constant. Special attention is drawn to the localized case, characterized by small values of x where some analytic predictions obtained using supersymmetric calculus exist [26,27].

The interest in such a study is twofold. First, it is interesting to see how the parametric properties of the system follow the transition between different pure universality classes. Second, the results obtained in the HBRM model may serve in the future as a reference for a comparison with statistics obtained in real physical systems. It is then of utmost importance to know what one may expect from the purely random model. This may enable one to isolate the nongeneric, i.e., characteristic for a given system, properties.

The paper is organized as follows. In the next section we describe the model and the parametric dynamics. The distribution of level velocities $P(v)$ is analyzed in Sec. III. Level curvatures are discussed in Sec. IV. Section V is devoted to the velocity-velocity correlation function $C_v(\lambda)$. Section VI considers higher-order statistical measures. Finally, we discuss the consequences of the results obtained for various statistical measures in Sec. VII.

II. PARAMETRIC DYNAMICS FOR HERMITIAN BAND RANDOM MATRICES

Hermitian band random matrices are defined by

$$H_{ij} = (\xi_{ij}^R + i\xi_{ij}^I)\Theta(b - |i - j|), \quad i, j = 1, \dots, N, \quad (2.1)$$

where $\Theta()$ denotes the unit step function vanishing at the origin. Independent random variables ξ_{ij}^R and ξ_{ij}^I are distributed according to Gaussian distributions with the zero-mean root-mean-square values equal to σ_{ij}^R and σ_{ij}^I , respectively. The parameter α measures the relative size of the imaginary part of the off-diagonal matrix elements $\alpha = (\sigma_{ij}^I/\sigma_{ij}^R)^2$, $i \neq j$ (the notation has been simplified with respect to Ref. [30]). A normalization condition $\text{Tr}(H^2) = N + 1$ keeps all the eigenvalues in a constrained energy range. It also allows us to express the variances of the real and imaginary parts of matrix elements in terms of matrix size N , integer bandwidth b , and real parameter α ,

$$(\sigma_{ij}^R)^2 = \frac{(N+1)}{2N + (\alpha+1)(2N-b)(b-1)}(1 + \delta_{ij}), \quad (2.2)$$

$$(\sigma_{ij}^I)^2 = \frac{\alpha(N+1)}{2N + (\alpha+1)(2N-b)(b-1)}(1 - \delta_{ij}). \quad (2.3)$$

For a diagonal random matrix ($b=1$) the density of eigenvalues is Gaussian and the level spacings are distributed according to the Poisson distribution, independently of the parameter α . In the opposite limiting case of the full matrix ($b=N$), variations of the parameter α correspond to the process of the time-reversal symmetry breaking in a dynamical system and control the transition between orthogonal ($\alpha=0$) and unitary ($\alpha=1$) ensembles.

Statistical properties of the spectrum and eigenvectors of real symmetric band matrices depend only on a scaling parameter $x = b^2/N$. This scaling law, observed initially by numerical computation of the localization length [28], was reported to describe also the distribution of eigenvalues [31] and eigenvectors [32] and was subsequently explained theoretically [33].

The same scaling law holds also for Hermitian matrices [33,34]. Moreover, effects of the time-reversal symmetry breaking are controlled by another scaling parameter $y = 2N\alpha/(1-\alpha)$ [30], stemming from the universal properties of the orthogonal-unitary transition founded by Pandey and Mehta [29]. The structure of eigenfunctions of HBRMs and the distribution of the inverse participation ratio have also been studied recently [35].

Let us now consider the parametric random matrix

$$H(\lambda) = H_1 \cos \lambda + H_2 \sin \lambda. \quad (2.4)$$

Both matrices H_1 and H_2 are taken from the same ensemble of HBRMs. Hence the spectral properties of H are stationary and do not depend on λ . Moreover, during the transition, the motion of eigenvalues is restricted to a bounded energy interval for arbitrary λ . This model of parametric dynamics was already used for the investigation of level curvatures [11] and velocity correlation functions [16,17]. The dynamics of eigenvalues as a function of λ may be treated as the dynamics of interacting particles (eigenvalues) with λ playing the role of fictitious time [2]. This allows us to interpret the slope of the levels as the velocity of the particles and their curvature as the corresponding accelerations.

Parametric dynamics defined above can be studied numerically in a straightforward way. For several values of ensemble parameters (N, b, α) we have generated random

matrices according to Eqs. (2.1)–(2.4). Diagonalizations of resulting matrices for several values of λ have allowed us then to find level velocities and curvatures by a finite-difference method. Special attention has been paid to obtain reliable values of velocities and curvatures, especially for very small and very large values, by varying the size of the step in λ [36]. Before computing the derivatives of the eigenvalues with respect to λ , the standard unfolding technique was applied [3] to set the mean level spacing Δ to unity. We have considered matrices of size N varying between 50 and 500, velocities and curvatures have been computed at about 200 different values of λ , and the typical number of independent realizations of the dynamics [Eq. (2.4)] in each case studied has varied with matrix size to ensure at least 200 000 data points in each statistics. In other words, we have simultaneously performed the averaging over the energy (data from different energy levels of a given matrix H) and the averaging over the disorder parameter (several realizations of the dynamics for the same values of N, b , and α).

To check the reliability of the numerical procedure we have set $b=N$ and we have reproduced known results concerning the distribution of velocities and curvatures as well as the velocity correlation function for the GOE ($\alpha=0$) and the GUE ($\alpha=1$). Moreover, we have verified that both scaling parameters x and y correctly describe the parametric dynamics. The statistical properties of all quantities studied have been found to be independent of the matrix dimension N (for sufficiently large N) provided the parameters x and y have been kept constant.

In the following sections we describe results obtained for different statistics, commencing with the distribution of first derivatives, i.e., velocities. To avoid any misunderstanding, let us repeat again that all the data presented are obtained for perpendicular transitions [both H_1 and H_2 in Eq. (2.4) belong to the *same* random matrix ensemble] as exemplified by double-sided arrows in Fig. 1. Thus, for all values of λ the scaling parameters x and y have the same values. We shall not consider here the case when the parameter change modifies the global symmetry properties, a situation exemplified by broken line arrow in Fig. 1.

III. DISTRIBUTION OF LEVEL VELOCITIES

For level dynamics within the GOE or the GUE the distribution of level velocities $P(v)$ is Gaussian [8,11,14]. This fact is easy to explain using first-order perturbation theory. For $\lambda=0$ the derivative $dE_i/d\lambda$ is equal to the diagonal element of matrix H_2 expanded in the eigenbasis of H_1 . Since both matrices are drawn independently from the same ensemble, the matrix elements are Gaussian random numbers leading to the Gaussian velocity distribution.

On the other hand, in the strongly localized limit an analytical formula for $P(v)$ given by Fyodorov [26] for systems with a broken TRI symmetry strongly differs from a Gaussian. A non-Gaussian character of the velocity distribution for the GOE to GUE transition, corresponding to the TRI symmetry breaking, has been discussed in [23–25].

We have analyzed the transition between localized and delocalized spectra both for random systems with a broken TRI symmetry (i.e., the ensembles interpolating between the

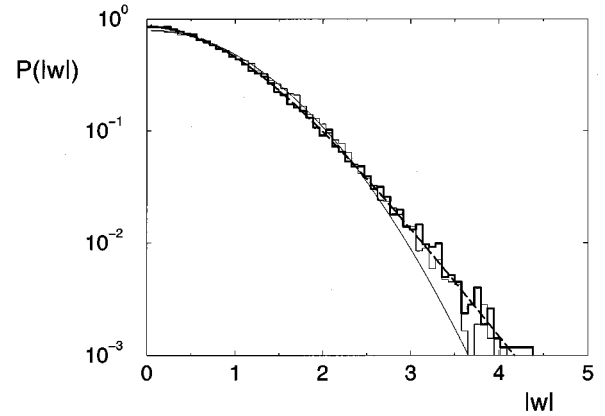


FIG. 2. Velocity distribution in a semilogarithmic scale for the HBRM model interpolating between the Poisson ensemble and the GUE ($\alpha=1$, a fully broken TRI symmetry). The thick (thin) line histogram corresponds to numerical data obtained in the localized case $x=0.126$ (the delocalized case $x=1.408$) from diagonalizations of 10 000 matrices of rank $N=71$. A dashed thick line represents the theoretical prediction, Eq. (3.1), while a thin line represents the Gaussian distribution.

Poisson ensemble and the GUE) and for ensembles interpolating between the Poisson ensemble and the GOE. The former allows us to test the analytical prediction of Fyodorov [26].

The theoretical prediction, as presented in [26], has no free parameters; both the shape of the distribution and its scale (determined by the velocity variance) are determined by the theory. Surprisingly, the direct comparison of that distribution with the numerical data obtained has been highly unsatisfactory. The agreement is recovered (see Fig. 2) when both the theoretical distribution and the numerically obtained data are rescaled with respect to the velocity variance $\sigma_v = \sqrt{\langle v^2 \rangle}$ (note that the mean velocity vanishes by the construction of the ensemble). Thus the apparent disagreement originally observed is due to the difference between the theoretical and numerically obtained values of the velocity variance (the ratio of the numerical value to the theoretical prediction being about 13). We do not have a clear explanation of this disagreement. It may be due to the fact that the bandwidth in our HBRM ensemble is sharply defined [compare Eq. (2.1)], while Fyodorov [26] assumed a smooth decrease of the random matrix elements variance with increasing distance from the diagonal $|i-j|$.

The theoretical prediction [26], represented by a smooth line in Fig. 2, takes the form

$$P(w) = \frac{\pi}{6} \frac{\pi w \coth(\pi w / \sqrt{6}) - \sqrt{6}}{\sinh^2(\pi w / \sqrt{6})}, \quad (3.1)$$

where the rescaled velocity $w = v / \sigma_v$. Similar qualitative agreement is obtained for different values of the scaling parameter up to x of the order of unity, corresponding to the transition to a delocalized case. Then the numerical data start to show a Gaussian (typical for the GUE) large velocity tail instead of the exponential tail corresponding to fully localized situation, as exemplified by the lack of large velocities in the numerical data presented in Fig. 2 as a thin line histogram.

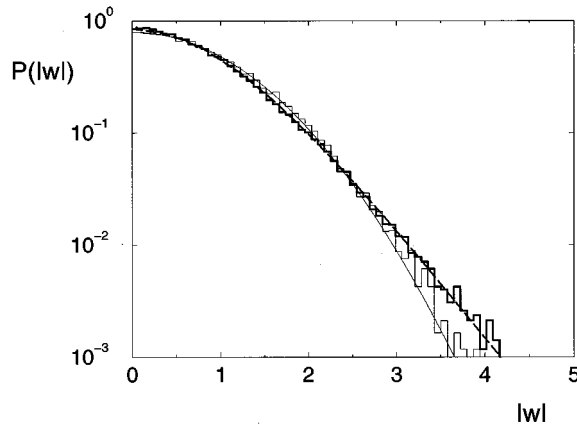


FIG. 3. Same as Fig. 2, but for real symmetric matrices $\alpha=0$: thick line histogram, a localized case $x=0.056$; thin line histogram, a delocalized case $x=5.63$.

Although the theoretical prediction is obtained for the case of a fully broken TRI symmetry, our numerical data indicate that it works extremely well also for preserved TRI symmetry (real symmetric matrices) provided that again the velocity variance is appropriately adjusted. The exemplary data are presented in Fig. 3 for two cases corresponding to strong localization and a transition to the delocalized regime. Here the numerically obtained variance is twice as large as the theoretical value calculated in the same way as for the broken-TRI-symmetry ensemble. It seems, therefore, that the same distribution, Eq. (3.1) describes the velocity distribution for both the TRI-symmetry case and the no-TRI-symmetry situation. The difference between the two ensembles (the former interpolating between the Poisson ensemble and the GOE, the latter between the Poisson ensemble and the GUE) appears in the numerical value of the velocity variance only. It is clear the variance is a unique parameter that determines the appropriate velocity scale, similarly as for the pure GOE and GUE [8].

IV. DISTRIBUTION OF LEVEL CURVATURES

Let us consider now the distribution of curvatures $K=d^2E/d\lambda^2$. As shown by Gaspard and co-workers [8], the tail of the distribution decays algebraically as $K^{-2-\beta}$. This universality has been verified for different systems [9–11]. At the same time, the small curvature behavior has been found to be nongeneric even for strongly chaotic systems [10,11] and reflecting the system-dependent wave-function localization properties (scarring by periodic orbits).

On the other hand, the scaled curvature

$$\kappa = K \frac{\Delta}{\beta \pi \sigma_v^2} \quad (4.1)$$

for pure random ensembles obeys the generalized Cauchy distribution [11–13]

$$P(\kappa) = N_\beta \frac{1}{(1 + \kappa^2)^{(\beta+2)/2}} \quad (4.2)$$

(where $\beta=1,2,4$ for the GOE, GUE, and GSE, respectively, and N_β denotes the normalization constant). Here we dem-

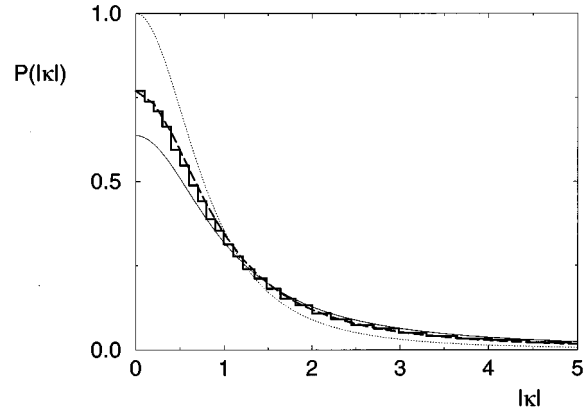


FIG. 4. Exemplary curvature distribution for the ensemble interpolating between the localized Poisson case ($\beta=0$) and the GOE ($\beta=1$) obtained numerically for matrices of rank $N=71$ and bandwidth $b=5$ corresponding to $x=0.352$ (histogram). The thick dashed line represents the fitted distribution, Eq. (4.2), with $\beta=0.59$. Thin solid and dotted lines represent the limiting distributions for the Poisson ensemble and the GOE, respectively.

onstrate that if one allows the parameter β to acquire real values $\beta \in (0,2]$, the same distribution may be used in a general case of the intermediate ensemble interpolating between Poisson ensemble, GOE, and GUE pure cases (provided we consider the perpendicular transition). The normalization constant is then equal to

$$N_\beta = \frac{1}{\sqrt{\pi}} \frac{\Gamma\left(\frac{\beta+2}{2}\right)}{\Gamma\left(\frac{\beta+1}{2}\right)} \quad (4.3)$$

and the rescaling Eq. (4.1) holds almost everywhere.

To test this conjecture we have generated several parametric dynamics perpendicular to crossovers between the Poisson ensemble and the GUE, the Poisson and between the GOE, and the GOE and the GUE using, as before, the formulation of Sec. II, Eqs. (2.1) and (2.4). The numerically obtained histograms of curvatures in the double-logarithmic scale have been used to fit the algebraic decay of the tail of the distribution by the formula $P(K) \sim K^{-\mu}$. Then β has been found as $\beta = \mu - 2$ [compare Eq. (4.2)]. The same value of β has been used together with the numerically obtained velocity variance to rescale the curvatures according to Eq. (4.1). The exemplary results of such a procedure together with the conjecture (4.2) are presented in Figs. 4 and 5 in double-linear and double-logarithmic scales, respectively. Observe the excellent agreement between the numerical results and the proposed distribution.

While Eq. (4.2) seems to describe well, at least approximately, the numerical data for curvatures everywhere in between pure cases of the GOE, the GUE, and the Poisson limit, the scaling (4.1) works best for the delocalized or weakly localized spectra. For the Poisson ensemble to GUE crossover, close to the Poisson limit, the scaling obtained using Eq. (4.1) is incorrect. The agreement with the generalized Cauchy distribution (4.2) is obtained only if the numerical data are rescaled additionally by a numerical factor of the

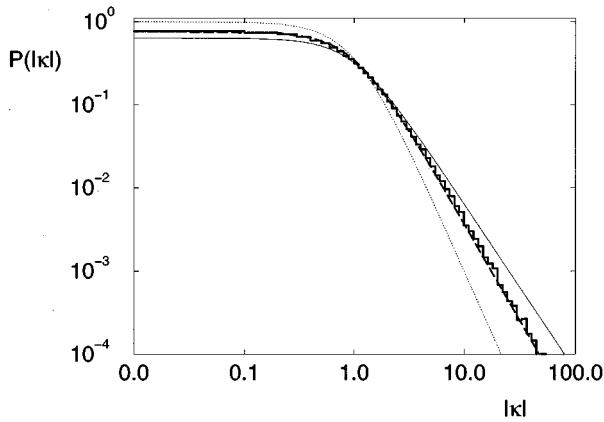


FIG. 5. Same as Fig. 4, but in a double-logarithmic scale.

order of unity (typically 1.5–2, depending on β). Putting it differently, the parameter β in the denominator of Eq. (4.1) should be replaced by another function of β that goes to β when the transition to the delocalized TRI-symmetry-broken case (i.e., the GUE) is fully accomplished. This indicates that the proposed distribution (4.2) is most probably the approximate one only. Still, we find it quite remarkable that this simple analytic expression, with the proper rescaling, works so well for the interpolating ensembles.

Let us mention that the power of the algebraic tail behavior may be analytically related to the level repulsion parameter β by a simple consideration of 2×2 random matrices [8] yielding $\mu = \beta + 2$. A comparison of β values obtained from the tail of the distribution with β' values obtained from the independent fit of the Izrailev distribution $P_{\beta'}(s)$ [38] is presented in Fig. 6 in the whole interval of the intermediate- β values. The agreement is quite good (and of a similar quality to that obtained for the Fourier transform of the velocity-velocity correlation function) considering that both the spacing distribution $P_{\beta'}(s)$ and the proposed curvature distribution $P(\kappa)$ are most probably good approximations to the true distributions only.

It is worth noting that the distribution (4.2) works well for the ensemble interpolating between the GOE and the GUE

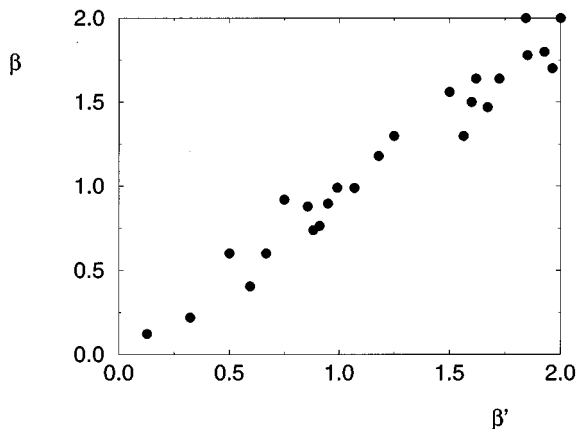


FIG. 6. Parameter β obtained from the decay of the tail of the curvature distribution against the level repulsion parameter β' obtained from the independent fit of the Izrailev distribution [38]. Each dot represents one ensemble interpolating between the Poisson ensemble, the GOE, or the GUE.

for the perpendicular action of the parameter λ . On the other hand, if λ is responsible for the TRI symmetry breaking, it has been shown that the tails of the curvature distribution are exponential [24,25] and not algebraic, as observed in this work. Parametric statistics are therefore sensitive to the way the parameter acts. Another example of this sensitivity is available from the earlier studies of periodic band random matrices [37] and three-dimensional Anderson model [39], where the curvature distribution close to a log-norm distribution has been observed in the localized case, while yet another distribution has been proposed in transition regime [40].

V. VELOCITY-VELOCITY CORRELATION FUNCTION

In a series of papers, Simons and Altshuler [14] have discussed the universality of parametric statistical properties for disordered samples as well as for Gaussian ensembles. To reveal the universality both the eigenvalues (to unit mean spacing) and the parameter λ (as $X = \sigma_v \lambda$) have to be rescaled [8,11,14]. We have observed the power of such a rescaling already in the previous sections.

Consider next the velocity-velocity correlation function, a frequent subject of recent investigations [14–18,21,24],

$$C_v(\lambda) := \frac{1}{2\pi\Delta^2} \left\langle \int_0^{2\pi} v_i(\lambda') v_i(\lambda' + \lambda) d\lambda' \right\rangle, \quad (5.1)$$

where $\langle \rangle$ denotes ensemble averaging and Δ stands for the mean level spacing. By definition $C_v(0) = \sigma_v^2$, thus the appropriately rescaled correlation functions take the form $\tilde{C}_v(X) = C_v(X) / \sigma_v^2$. Moreover, several models of time-reversal symmetry breaking due to the Aharonov-Bohm flux lead to a correlation function practically indistinguishable from the one characteristic for the GUE.

It was shown [14,21,15] that for all three universality classes the rescaled correlation function

$$C_v(X) \sim A_\beta X^{-2}, \quad X \rightarrow \infty, \quad (5.2)$$

with the proportionality coefficient A_β dependent on the ensemble (we denote by β the level repulsion parameter $\beta = 1, 2, 4$ for the GOE, the GUE, and the GSE, respectively).

Explicit expressions have been obtained [14] for closely related [but distinct from $C_v(\lambda)$] autocorrelation functions at fixed energy. A global approximation for $\tilde{C}_v(X)$ has been proposed [16]. For the case of a classically chaotic system subject to an Aharonov-Bohm flux Berry and Keating [22] obtained a semiclassical approximation for $C_v(\lambda)$ having the form of an everywhere analytic function of λ . Yet it was demonstrated [17] that $C_v(\lambda)$ is not analytic and suffers a logarithmic singularity at $\lambda = 0$.

Analytic properties of correlation functions are conveniently studied using the periodicity in λ . In the Fourier domain

$$C_v(\lambda) = \sum_{n=0}^{\infty} c_n \cos(n\lambda). \quad (5.3)$$

The mean-squared velocity, determining the scale, is given by the sum of all coefficients $\sigma_v^2 = C(0) = \sum_{n=0}^{\infty} c_n$. Expand-

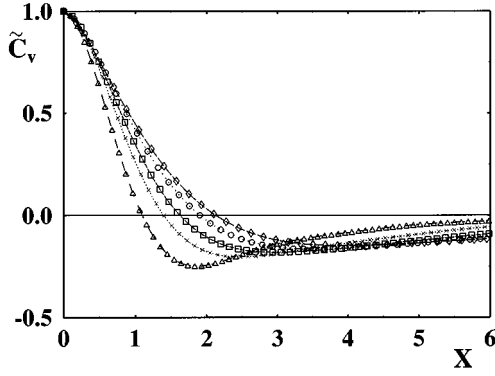


FIG. 7. Rescaled velocity correlation function $\tilde{C}_v(X)$ obtained for five transitions perpendicular to the GUE-Poisson crossover $N=71, c=2.0$: $b=71$ (Δ) (GUE), $b=10$ (+), $b=7$ (\square), $b=5$ (\circ), and $b=4$ (\diamond). Ensemble averaging is performed over 100 matrices; the lines are drawn to guide the eye.

ing the dependence of a given eigenvalue on λ in the Fourier series $E_i = \sum_{n=-\infty}^{\infty} a_n e^{in\lambda}$, where $a_n = a_n^*$, on account of Eq. (5.1) it is easy to see that $c_n = n^2 \langle |a_n|^2 \rangle / \Delta^2$.

The asymptotic behavior of $C_v(\lambda) \sim -\lambda^{-2}$ corresponds to a linear increase of Fourier coefficients c_n for small n . On the other hand, for large n it was shown [17] that $\langle |a_n|^2 \rangle \sim n^{-4-\beta}$ and, consequently,

$$c_n \sim n^{-2-\beta}. \quad (5.4)$$

This result was obtained by extending the parameter λ into the complex plane and analyzing the distribution of branch points and anticrossings [4,6].

Thus, despite the nonanalytic character of the correlation function, both $C_v(\lambda)$ and its Fourier transform have simple asymptotics given by Eqs. (5.2) and (5.4), respectively. It is interesting to see whether a similar behavior may be found for the interpolating ensembles. To this end we have studied the asymptotics of C_v for all three possible transitions, i.e., ensembles interpolating between the Poisson ensemble and the GOE, the Poisson ensemble and the GUE, as well as the GOE and the GUE. In all cases the parameter λ acted perpendicular to a given transition (compare Fig. 1).

We have observed the same X^{-2} large- X behavior Eq. (5.2) independently of the ensemble studied. As an example Fig. 7 shows the rescaled velocity-velocity correlation functions $\tilde{C}_v(X)$ corresponding to five different cases along the Poisson-GUE crossover.

Algebraic decay of the corresponding Fourier transforms is visualized in Fig. 8. Observe the continuous change of the slope, growing from -4 for the GUE until -2 for the Poisson limit. This corresponds to the continuous change of the repulsion parameter β between 2 and 0 in the level spacing distribution. Independently one may fit the nearest-neighbor spacing distribution obtained numerically to the Izrailev distribution [38] $P_{\beta'}(s)$, which provides an excellent approximation for the nearest-neighbor spacing distribution for the interpolating ensembles. $P_{\beta'}(s) \sim s^{\beta'}$ for small s . We have verified that β values obtained by fitting the straight line to the tail of $\log(c_n)$ equal β' values obtained from the fits of the spacing distribution within 5%. Therefore, we conclude

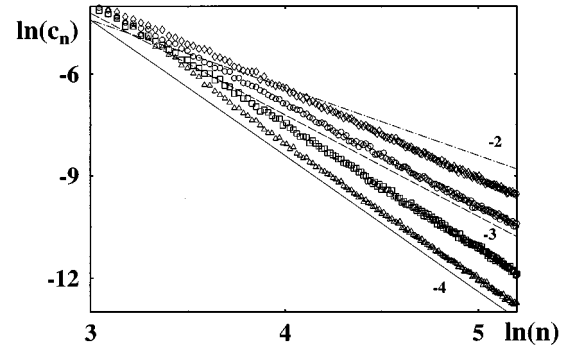


FIG. 8. Fourier transform of the velocity correlation functions displayed in Fig. 7 in the log-log scale. Lines represent slopes characteristic for the GUE (-4), the GOE (-3), and the Poisson ensemble (-2). The data for $b=10$ are not plotted to improve the legibility of the figure.

that the validity of Eqs. (5.2) and (5.4) extends to the intermediate ensembles and fractional values of the repulsion parameter β .

We stress again that this result is restricted to the perpendicular transitions only. If parameter λ is responsible for the transition between the ensembles (e.g., the magnetic flux in the Aharonov-Bohm effect) the velocity-velocity correlation function obeys the $c_n \sim n^{-4}$ algebraic decay, independently of the degree of localization [17]. Thus, similarly to the velocity distribution itself [23], also the velocity-velocity correlation function $\tilde{C}_v(X)$ is sensitive to the nature of perturbation generating the parametric dynamics.

In a full analogy with the velocity-velocity correlation function (5.1) we define the curvature correlation function

$$C_k(\lambda) := \frac{1}{2\pi\Delta^2} \left\langle \int_0^{2\pi} K_i(\lambda') K_i(\lambda' + \lambda) d\lambda' \right\rangle. \quad (5.5)$$

However, this function does not provide us with any new information. This fact is easy to understand studying the Fourier expansion $C_k(\lambda) = \sum_{n=0}^{\infty} k_n e^{in\lambda}$. As for velocity correlation function one uses mean Fourier coefficients of individual energy levels and obtains relation $k_n = n^4 \langle |a_n|^2 \rangle / \Delta^2$. A comparison with the velocity correlation function Fourier coefficients yields immediately

$$C_k(\lambda) = \frac{\partial^2}{\partial \lambda^2} C_v(\lambda), \quad (5.6)$$

which easily yields the properties of $C_k(\lambda)$ from known properties (e.g., the asymptotic behavior) of $C_v(\lambda)$. Equation (5.6) holds for an arbitrary matrix ensemble. For completeness we present the numerically obtained $C_k(\lambda)$, rescaled with respect to $C_k(0)$, for the GOE and the GUE in Fig. 9. Notice a much faster decay of the correlation between curvatures as compared to the velocity correlation function. Asymptotically, using $C_v \sim X^{-2}$ and Eq. (5.6) we get $C_k \propto X^{-4}$ for the large rescaled parameter X , in full agreement with Fig. 9. The curvature correlation function, in view of Eq. (5.6), may be used, together with the velocity correlation function, for numerical tests of the accuracy of the curvature evaluation (which may be quite tricky using the finite-

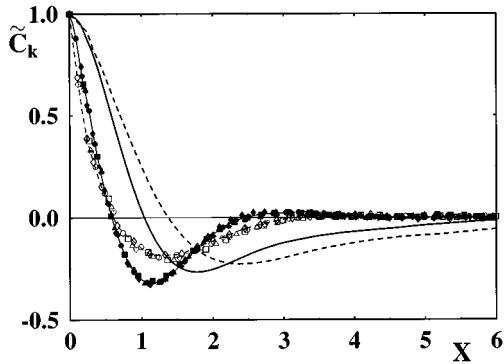


FIG. 9. Curvature-curvature correlation function $\tilde{C}_k(X)$ obtained for $N=50$ (\diamond), 60 (\circ), 70 (\square), 80 (\triangle), and $N=90$ (\heartsuit/\clubsuit) for the GOE (open symbols) and the GUE (full symbols). Universal rescaled velocity correlations are represented for comparison by thick dashed (GOE) and solid (GUE) lines.

difference method since small and large curvatures may require different steps in the parameter).

VI. HIGHER DERIVATIVES OF ENERGY WITH RESPECT TO THE PARAMETER

Algebraic decay of the Fourier transform of the velocity correlation function, on the one hand, provides information about the singularity of some higher derivative of $C_v(\lambda)$ at $\lambda=0$ and, on the other hand, indicates the possibility of a divergence of a distribution variance of some higher derivatives of the energy levels with respect to the parameter [17]. In particular, for the orthogonal ensemble ($\beta=1$), the variance of the curvature distribution $\langle K^2 \rangle$ does not exist and in order to characterize the mean curvature one uses the mean absolute value $\langle |K| \rangle$ instead [37]. Moreover, the second moment of the distribution of the third derivatives of energy levels $L := d^3 E / d\lambda^3$ was predicted [17] to diverge for $\beta=1$ and $\beta=2$.

To test this prediction we have studied the distribution of these third derivatives. The most difficult part here is to determine what to call them, using the level motion picture where the curvature of the level is identified with the acceleration of the fictitious particle, the third derivative of the energy will correspond to the derivative of the acceleration. In the spirit of this mechanical analogy we refer to the third derivative as a change in acceleration.

We have restricted the numerical study of the distribution of the third derivatives to canonical orthogonal and unitary ensembles (the GOE and GUE). The obtained numerical results are displayed in Fig. 10. As expected, the distributions of the third derivatives are characterized by the algebraic tails; the numerically obtained power-law decay yields $P(L) \sim L^{-(\beta+3/2)}$, which confirms the divergence of the variances both for the GOE and the GUE.

It is interesting that the distribution of the third derivatives may be quite nicely approximated by a very simple ansatz

$$P(L) = \frac{\mathcal{N}'_\beta}{(1 + B_\beta L^{A(\beta)})^{(\beta+3)/2A(\beta)}}, \quad (6.1)$$

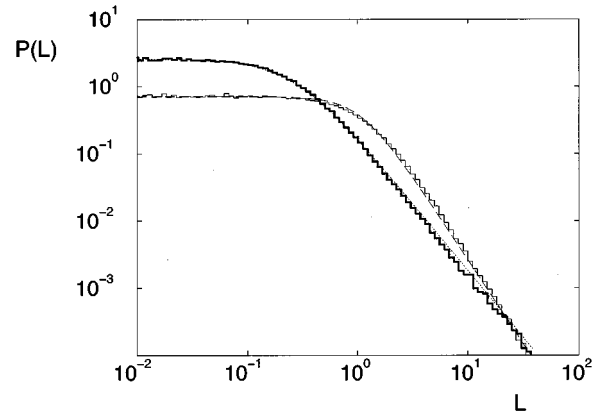


FIG. 10. Distribution of third derivatives of the eigenenergy with respect to the parameter $P(L)$ in the double-logarithmic scale. Histograms correspond to numerically obtained data for the GOE (thick line) and the GUE (thin line), both obtained for random matrices of rank $N=71$. Dotted and dashed lines represent the best fit of the proposed distribution, Eq. (6.1), for the GOE and the GUE, respectively.

where \mathcal{N}'_β is a normalization constant and B_β and $A(\beta)$ are free parameters. In Eq. (6.1) the third derivatives are conveniently rescaled taking the unfolded spectrum (i.e., with the mean level spacing equal to unity) with derivatives calculated with respect to the rescaled parameter $X = \sqrt{\langle v^2 \rangle} \lambda$.

We have fitted the distribution of this form to the numerical data for both the GOE and the GUE. The results are represented in Fig. 10 as smooth curves and quite successfully represent the numerical data. The obtained values of the parameters are equal for the GOE to $A_1=1.67$ and $B_1=9.08$, while for the GUE we obtain $A_2=2.50$ and $B_2=0.84$. The obtained values of A_β are close to simple fractions $A_1=5/3$ and $A_2=5/2$, the corresponding curves are indistinguishable from best fits within the accuracy of our data.

VII. CONCLUDING REMARKS

We have analyzed various aspects of parametric dynamics in the space of Hermitian random matrices. Such a model may be applied to study transitions between Poissonian, orthogonal, and unitary universality classes. We have analyzed numerically the situations when the parameter change does not modify the global properties of the ensemble studied, the case labeled as a ‘‘perpendicular’’ transition to contrast it with the ‘‘parallel’’ case when the parameter is responsible for the breakup of the symmetry or other change of the properties of the ensemble studied. We have, however, compared our results with predictions of other works where often such a parallel parameter action was considered.

We have paid particular attention to the study of the transition between the Poissonian ensemble characterized by strongly localized wave functions and the delocalized Gaussian ensembles (the GOE or GUE). In particular, the numerical tests of the analytic predictions for the distribution of level velocities in the case of broken time-reversal invariance [26] confirmed the predicted shape. We have observed a disagreement between the theory [26] and the numerical data, however, as far as the prediction for the velocity variance is

considered. We have discussed the possible origin of this difference. We have shown that the distribution of the same functional form works for the delocalization transition also for the real symmetric random matrices. This calls for the extension of the theory to such a case.

We have studied in detail also the distribution of level curvatures. Here no analytic prediction is available. We have found that the numerically obtained distribution of curvatures is well approximated by the generalized Cauchy distribution (4.2) shown earlier to be exact [11–13] for the canonical ensemble, the GOE, and the GUE. The only required modification is to take the fractional value of the level repulsion parameter β in accordance with the spacing distribution. We have found also that the same rescaling (4.1) holds everywhere except for the localized, no-TRI-symmetry ensemble. Then the agreement with Eq. (4.2) requires additional multiplication of all curvatures (rescaling) by a factor of the order of unity and dependent on β .

This form of the curvature distribution implies its algebraic tails of the form $P(K) \sim K^{-2-\beta}$. Similarly, we have found that the same level repulsion parameter β governs the tails of the Fourier-transformed velocity correlation functions. Explicitly, the corresponding Fourier coefficients satisfy to a good precision $c_n \sim n^{-2-\beta}$.

A comparison with other works, where mostly the parallel transition have been studied [23–25,35,37,39] in various models, indicates strong differences with the parallel transitions. This difference has been observed for the velocity correlation function in the case of a partially broken TRI symmetry in a fully delocalized case [23]. Here we have shown that the sensitivity of level dynamics to the way in which the parameter acts extends also to other parametric statistical measures as well as to other ensembles interpolating between ‘‘pure’’ cases of the Poisson ensemble, the GOE, and the GUE. This has an important consequence: it shows that the universality of parametric dynamics is more limited than anticipated before [14].

Finally consider the consequence of the presented results for studies of realistic systems. Consider the semiclassical limit when the system is ‘‘large,’’ with a high density of states and many highly excited levels. In the generic situation a small change of the parameter cannot induce significant changes in system symmetries and global properties; small changes of a parameter may be thus considered as perpendicular cases. This indicates that the perpendicular

transitions studied in this paper are typically generic. An important exception is the change of the magnetic fields in systems with no additional symmetries where the field induces the breakup of the time-reversal symmetry acting, therefore, in a parallel way.

Thus the fact that the curvature distribution for the transition between the Poisson ensemble and the GOE, realized via the banded matrix model studied here, is described by the generalized Cauchy law Eq. (4.2) has important consequences. It has been suggested (see [30] and references cited therein) that banded matrices may be used to simulate statistical properties of partially chaotic systems interpolating between the integrable case (with Poisson level spacing statistics) and the fully chaotic case (the GOE). This has been partially based on the similarity of the level spacing distribution observed in both cases, well approximated by the Izrailev ansatz [38] or for TRI symmetry systems by the Brody distribution. However, even for chaotic systems, as shown before, small curvature behavior may be abundant due to isolated avoided crossings and scarring of wave functions [11]. For the mixed-phase-space systems the avoided crossings are typically quite narrow and isolated, between them the levels can be adiabatically followed as a parameter is varied. Generically, small changes of a parameter are accompanied by small changes of eigenenergies that may be treated by a Taylor-series expansion with a leading linear term. It shows that such systems will exhibit a great abundance of small curvatures, accompanied possibly by a singularity of the distribution at $K=0$ (see also [11] for an additional discussion and numerical examples). Banded random matrices show a curvature distribution different from what is expected for a quantum system with a mixed phase space. Thus this ensemble is not adequate for simulating the statistical properties of partially integrable or weakly chaotic systems at least in cases when parametric dynamics is concerned. On the other hand, the HBRM ensemble seems to be very useful for obtaining predictions for random systems that exhibit a transition to localization, well into the localization regime.

ACKNOWLEDGMENTS

It is a pleasure to thank Italo Guarneri and Yan Fyodorov for fruitful discussions. We acknowledge financial support from Polish Committee of Scientific Research under Grant No. 2P03B 03810.

[1] M. L. Mehta, *Random Matrices*, 2nd ed. (Academic, New York, 1991).
 [2] F. Haake, *Quantum Signatures of Chaos* (Springer, Berlin, 1991).
 [3] O. Bohigas, in *Chaos and Quantum Physics*, Proceedings of the Les Houches Summer School of Theoretical Physics, Session LII, edited by M.-J. Giannoni, A. Voros, and J. Zinn-Justin (North-Holland, Amsterdam, 1991).
 [4] M. Wilkinson, *J. Phys. A* **22**, 2795 (1989).
 [5] J. Goldberg and W. Schweizer, *J. Phys. A* **24**, 2785 (1991).
 [6] J. Zakrzewski and M. Kuś, *Phys. Rev. Lett.* **67**, 2749 (1991); J.

Zakrzewski, D. Delande, and M. Kuś, *Phys. Rev. E* **47**, 1665 (1993).
 [7] J. Goldberg, U. Smilansky, M. V. Berry, W. Schweizer, G. Wunner, and G. Zeller, *Nonlinearity* **4**, 1 (1991).
 [8] P. Gaspard, S. A. Rice, and K. Nakamura, *Phys. Rev. Lett.* **63**, 930 (1989); P. Gaspard, S. A. Rice, H. J. Mikeska, and K. Nakamura, *Phys. Rev. A* **42**, 4015 (1990).
 [9] D. Saher, F. Haake, and P. Gaspard, *Phys. Rev. A* **44**, 7841 (1991).
 [10] T. Takami and H. Hasegawa, *Phys. Rev. Lett.* **68**, 419 (1992).
 [11] J. Zakrzewski and D. Delande, *Phys. Rev. E* **47**, 1650 (1993).

- [12] F. von Oppen, *Phys. Rev. Lett.* **73**, 798 (1994).
- [13] Y. Fyodorov and H. J. Sommers, *Phys. Rev. E* **51**, 2719 (1995); *Z. Phys. B* **99**, 123 (1995).
- [14] B. D. Simons and B. L. Altshuler, *Phys. Rev. Lett.* **70**, 4063 (1993); *Phys. Rev. B* **48**, 5422 (1993).
- [15] C. W. J. Beenakker, *Phys. Rev. Lett.* **70**, 4126 (1993); C. W. J. Beenakker and B. Rejaei, *Physica A* **203**, 61 (1994).
- [16] J. Zakrzewski, *Z. Phys. B* **98**, 273 (1995).
- [17] I. Guarneri, K. Życzkowski, J. Zakrzewski, L. Molinari, and G. Casati, *Phys. Rev. E* **52**, 2220 (1995).
- [18] H. Bruus, C. H. Lewenkopf, and E. R. Mucciolo, *Phys. Rev. B* **53**, 9968 (1996).
- [19] P. Seba, K. Życzkowski, and J. Zakrzewski, *Phys. Rev. E* **54**, 2438 (1996).
- [20] J. Zakrzewski, K. Dupret, and D. Delande, *Phys. Rev. Lett.* **74**, 522 (1995).
- [21] A. Szafer and B. L. Altshuler, *Phys. Rev. Lett.* **70**, 587 (1993).
- [22] M. V. Berry and J. P. Keating, *J. Phys. A* **27**, 6167 (1994).
- [23] N. Taniguchi, A. Hashimoto, B. D. Simons, and B. L. Altshuler, *Europhys. Lett.* **27**, 335 (1994).
- [24] A. Kamenev and D. Braun, *J. Phys. (France) I* **4**, 1049 (1994).
- [25] D. Braun and G. Montambaux, *Phys. Rev. B* **50**, 7776 (1994).
- [26] Y. V. Fyodorov, *Phys. Rev. Lett.* **73**, 2688 (1994).
- [27] Y. V. Fyodorov and A. D. Mirlin, *Phys. Rev. B* **51**, 13 403 (1995).
- [28] G. Casati, L. Molinari, and F. Izrailev, *Phys. Rev. Lett.* **64**, 1851 (1990).
- [29] A. Pandey and M. L. Mehta, *Commun. Math. Phys.* **16**, 2655 (1983).
- [30] K. Życzkowski and R. Serwicki, *Z. Phys. B* **99**, 449 (1996).
- [31] G. Casati, F. Izrailev, and L. Molinari, *J. Phys. A* **24**, 4755 (1991).
- [32] K. Życzkowski, M. Lewenstein, M. Kuś, and F. M. Izrailev, *Phys. Rev. A* **45**, 811 (1992).
- [33] Y. V. Fyodorov and A. D. Mirlin, *Phys. Rev. Lett.* **67**, 2405 (1991).
- [34] K. Życzkowski, *Acta Phys. Pol. B* **24**, 967 (1993).
- [35] F. Izrailev, L. Molinari, and K. Życzkowski, *J. Phys. (France) I* **6**, 455 (1996).
- [36] P. Kunstman, Master thesis, Uniwersytet Jagiélłonski, 1995 (unpublished).
- [37] G. Casati, I. Guarneri, F. Izrailev, L. Molinari, and K. Życzkowski, *Phys. Rev. Lett.* **72**, 2697 (1994).
- [38] F. Izrailev, *Phys. Rep.* **129**, 299 (1990).
- [39] K. Życzkowski, F. Izrailev, and L. Molinari, *J. Phys. (France) I* **4**, 1469 (1994).
- [40] C. M. Canali, C. Basu, W. Stephan, and V. E. Kravtsov (unpublished).